Solution processable liquid metal nanodroplets by surface-initiated atom transfer radical polymerization

Jiajun Yan¹, Mohammad H. Malakooti², Zhao Lu³, Zongyu Wang¹, Navid Kazem⁴, Chengfeng Pan², Michael R. Bockstaller³, Carmel Majidi^{2,4} and Krzysztof Matyjaszewski¹

Eutectic gallium indium (EGaIn) is a liquid metal allov at room temperature. EGaIn microdroplets can be incorporated into elastomers to fabricate highly stretchable, mechanically robust, soft multifunctional composites with high thermal stability1 and electrical conductivity2-4 that are suitable for applications in soft robotics and self-healing electronics⁵⁻⁷. However, the current methods of preparation rely on mechanical mixing, which may lead to irregularly shaped micrometresized droplets and an anisotropic distribution of properties8. Therefore, procedures for the stabilization of sub-micrometre-sized droplets of EGaIn and compatibilization in polymer matrices and solvents have attracted significant attention9-12. Here we report the synthesis of EGaIn nanodroplets stabilized by polymeric ligand encapsulation. We use a surface-initiated atom transfer radical polymerization initiator to covalently functionalize the oxide layer on the surface of the EGaIn nanodroplets¹³ with poly(methyl methacrylate) (PMMA), poly(n-butyl acrylate) (PBMA), poly(2-dimethylamino)ethyl methacrylate) (PDMAEMA) and poly(n-butyl acrylate-blockmethyl methacrylate) (PBA-b-PMMA). These nanodroplets are stable in organic solvents, in water or in polymer matrices up to 50 wt% concentration, enabling direct solution-casting into flexible hybrid materials. The liquid metal can be recovered from dispersion by acid treatment. The nanodroplets show good mechanical, thermal and optical properties, with a remarkable suppression of crystallization and melting temperatures (down to -80 °C from 15 °C).

We use a recently developed universal tetherable initiator for metal oxide surfaces¹⁴, which permits surface-initiated atom transfer radical polymerization (SI-ATRP) from a broad spectrum of metal surfaces. EGaIn droplets were first modified under ultrasonication in tetrahydrofuran by 12-(2-bromoisobutyramido)dodecanoic acid (BiBADA) followed by SI-ATRP (Fig. 1a–d). Under ultrasonic agitation, EGaIn was dispersed into sub-micrometre-sized droplets and an oxide layer formed on the surface of the droplets¹⁵, allowing attachment of BiBADA to the surface. After modification, the mixture was washed with tetrahydrofuran using cycles of centrifugation–ultrasonication to produce a grey paste-like product (Fig. 1e). Polymerization of methyl methacrylate (MMA) was performed via ATRP from the initiator-modified EGaIn droplets¹⁶. The resulting product was separated by precipitation in methanol as fibre-like polymer hybrid materials (Fig. 1f), which were redispersible in

organic solvents (Fig. 1g). We hypothesize that the coupling between polymer chains and metal surface proceeds via a thin 'oxide skin layer' that is known to form on the surface of EGaIn, which is supported by the finding that the liquid metal could be separated as a millimetre-sized droplet by acidification of dispersion accompanied by the disappearance of the grey colour in the dispersion (Fig. 1h).

Several cycles of centrifugation were required during the purification process. The high EGaIn density (>6 g ml⁻¹) and small-molecule nature of BiBADA led to phase separation and loss of EGaIn content. Therefore, a one-pot approach was employed (Fig. 1c). An adequate amount of BiBADA, 0.125 g ml⁻¹ EGaIn, was added to the polymerization solution as an in situ tetherable initiator. The reaction mixture was ultrasonicated overnight before adding an activator regenerator (copper wire or azo-initiator) and degassing. The EGaIn droplets formed during ultrasonication were covered by BiBADA in the polymerization solution. Once degassed, the tethered and free BiBADA simultaneously initiated the polymerization. In contrast to inorganic nanoparticles, the dynamic nature of EGaIn could lead to reorganization of the droplets and detachment/reat-tachment of the BiBADA initiators. The detailed results of polymerization kinetics are presented in Supplementary Figs. 3–5.

A series of EGaIn-polymer hybrid materials were prepared and characterized using the one-pot approach (Table 1). A relatively high dispersity of the obtained polymers is related to a strong reducing power of EGaIn itself (cf. kinetics discussion in the Supplementary Information).

We used transmission electron microscopy (TEM) to study the morphology of EGaIn-PMMA hybrid materials prepared by the two-step approach (Fig. 1f) with minimal free polymer content $(f_{\text{EGaIn}} = 8.4 \text{ wt\%})$. Nearly spherical droplets of EGaIn of ~200 nm were observed (Fig. 1i). A magnified TEM image showed the presence of a PMMA corona surrounding the EGaIn droplets (Fig. 1i, inset). In our attempts to determine the maximal amount of polymer-modified EGaIn nanodroplets dispersible in organic media, we observed no practical solubility limit of PMMA-tethered EGaIn nanodroplets in tetrahydrofuran, providing evidence of the high solubilizing efficacy of the tethered PMMA. This is in stark contrast to established small-molecule surfactant systems that only enable millimolar amounts of nanodroplets to be dispersed without inducing coalescence (Supplementary Fig. 1)9. The solubilizing efficacy was determined by quantitative analysis of the turbidity of EGaIn nanodroplet dispersions using a spectroscopic process reported

LETTERS

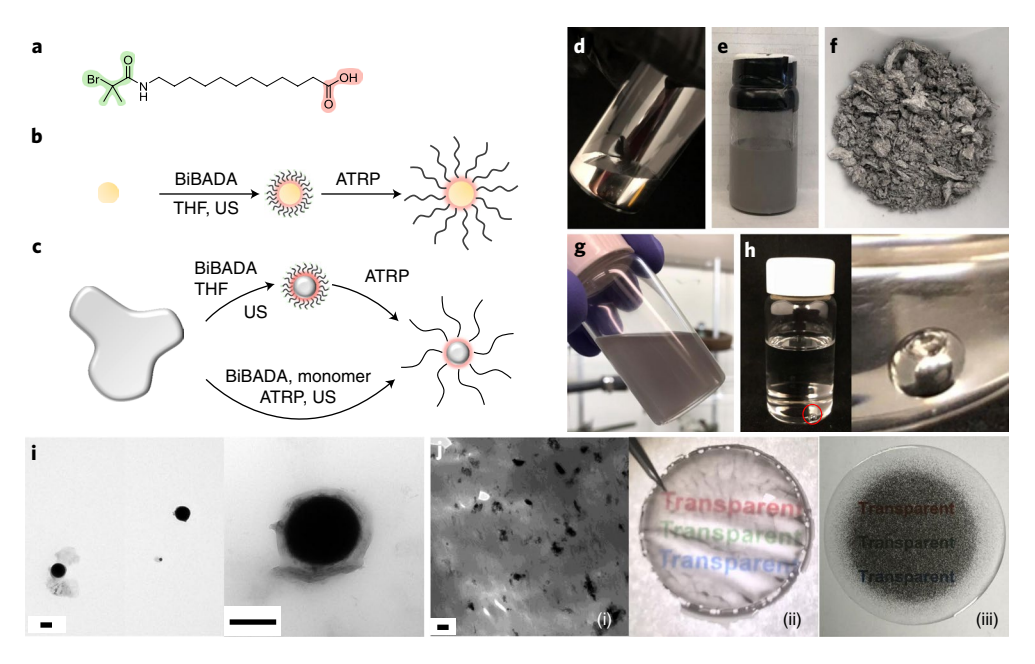


Fig. 1 | SI-ATRP from EGaln and EGaln-PMMA hybrid droplets. a, Structure of BiBADA. **b**, Two-step BiBADA-functionalized and SI-ATRP of nanoparticles. **c**, Stepwise functionalization of EGaln or SI-ATRP from in situ functionalized EGaln droplets. **d-h**, Photographs of pristine EGaln (**d**), BiBADA-functionalized EGaln droplets dispersed in tetrahydrofuran (**e**), precipitated poly(methyl methacrylate) (PMMA)-grafted EGaln droplets as polymeric fibres (**f**), redispersed PMMA-grafted EGaln droplets in tetrahydrofuran that have formed a homogeneous dispersion (**g**) and a free EGaln droplet observed after addition of three drops of 36% HCl solution (**h**). Inset (**h**), close-up image of the EGaln droplet. **i**, Transmission electron microscopy (TEM) images of PMMA-grafted EGaln droplets. **j**, (i) TEM image of microsectioned free-standing hybrid film of PMMA-grafted EGaln (scale bar, 200 nm); (ii) a 60-μm-thick free-standing film containing 10 wt% EGaln-PMMA hybrid material; (iii) EGaln/PDMS binary composite film containing 10 wt% of EGaln prepared using a mechanical planetary mixer. US, ultrasonication.

Table 1 | Composition, molecular weight, dispersity and inorganic fraction of representative EGaln-polymer hybrid materials prepared by the one-pot approach.

Entry	Polymer composition	M _n ^a	$M_{\rm w}/M_{\rm n}^{\rm a}$	f _{EGain} (wt%) ^b
1	PMMA ^c	8.13×10 ⁴	2.03	53.9
2	PDMAEMA ^d	1.03×10 ⁵	1.53	7.1
3	PBMA ^e	2.74×10^{5}	2.41	31.2
4	PBA ^f	9.78×10^{4}	2.45	33.5
5	PBA-b-PMMA ^g	1.38 × 10 ⁵	2.65	20.2

*Determined by size exclusion chromatography calibrated to linear PMMA standards using tetrahydrofuran or dimethylformamide (PDMAEMA only) as eluents. *Determined by thermogravimetric analysis as described in the Supplementary Information. *Reaction condition: [BiBADA] $_{\circ}$ [MMA] $_{\circ}$ [CuBr $_{\circ}$] $_{\circ}$ /[AlBN] $_{\circ}$ [Me $_{\circ}$ TREN] $_{\circ}$ =1/400/0.1/0.3/0.5; EGaln/BiBADA=1/8 (vol/wt); anisole=50 vol%; 50 °C sonication bath; PMMA, poly(methyl methacrylate). *Reaction condition: [BiBADA] $_{\circ}$ /[DMAEMA] $_{\circ}$ /[CuBr $_{\circ}$] $_{\circ}$ /[V-501] $_{\circ}$ /[Me $_{\circ}$ TREN] $_{\circ}$ =1/1000/0.1/0.3/0.5; EGaln/BiBADA=1/8 (vol/wt); MeCN=50 vol%; 50 °C sonication bath; PDMAEMA, poly(2-dimethylamino)ethyl methacrylate). *Reaction condition: [BiBADA] $_{\circ}$ /[EuBr $_{\circ}$] $_{\circ}$ /[AlBN] $_{\circ}$ /[Me $_{\circ}$ TREN] $_{\circ}$ =1/1000/0.1/0.5/0.5; EGaln/BiBADA=1/8 (vol/wt); anisole=50 vol%; 50 °C sonication bath; PBMA, poly(n-butyl methacrylate). *Reaction condition: [BiBADA] $_{\circ}$ /[EuBr $_{\circ}$] $_{\circ}$ /[Me $_{\circ}$ TREN] $_{\circ}$ =1/1000/0.1/0.5; EGaln/BiBADA=1/8 (vol/wt); Ø1 mm × 5 cm copper wire; anisole=50 vol%; 50 °C sonication bath; PBA, poly(n-butyl acrylate). *Reaction condition: [EGaln-g-PBA-Br] $_{\circ}$ /[MMA] $_{\circ}$ /[CuBr $_{\circ}$] $_{\circ}$ /[AlBN] $_{\circ}$ /[Me $_{\circ}$ TREN] $_{\circ}$ =1/500/0.1/0.5/0.5; anisole=75 vol%; 50 °C sonication bath.

previously⁹. The analysis revealed that polymer-modification increased the dispersion limit of EGaIn nanodroplets in organic solvents by more than an order of magnitude. For example, in the case of PMMA-tethered EGaIn, dispersions in tetrahydrofuran with 1.5 mM metal content were stable for one week (the longest time tested in our experiments) while small-molecule surfactant systems

did show droplet coalescence and precipitation after 24h at concentrations of <0.17 mM. A control experiment with ATRP in the presence of EGaIn and a small amount of surfactants indicated that covalent attachment of the polymer brushes to EGaIn nanodroplets was a critical factor (Supplementary Fig. 2).

The high solubilizing efficacy enabled the direct film casting of free-standing EGaIn–PMMA hybrid films from tetrahydrofuran solution. No polymer needed to be admixed, thus rendering the material a one-component hybrid. Microtomic TEM images of the free-standing film confirmed the presence of well dispersed EGaIn nanodroplets (Fig. 1j(i)). A pertinent feature of the one-component hybrid is shown in Fig. 1j(ii),(iii), which compares the optical appearance of EGaIn–PMMA with a classical EGaIn/PDMS binary composite film of analogous metal content prepared by mechanical dispersion. The figures demonstrate that the uniform microstructure (in conjunction with droplet size in the nanometre range) of EGaIn–PMMA renders materials near transparent, whereas binary hybrids (with ~10–50 μ m droplets) of analogous composition are opaque¹⁷.

In comparison to PMMA, poly(n-butyl methacrylate) (PBMA) has a much lower glass transition temperature $T_{\rm g}~(\sim 20~{\rm C})^{18}$. Therefore, its mechanical behaviour lies within the rubbery plateau at room temperature, due to polymer chain entanglement¹⁹. TEM images of the EGaIn–PBMA hybrid materials show the presence of nearly uniform 120 nm spherical droplets in the supernatant after the larger droplets were allowed to settle for 24 h in a tetrahydrofuran dispersion (Fig. 2a). To illustrate the versatility of the presented approach, the unpurified hybrid materials were directly cast into tensile test specimens from the tetrahydrofuran dispersion. TEM images of microtomed sections showed slightly elongated EGaIn droplets with a size distribution range from <100 nm to a few hundred nanometres (Fig. 2b). The as-cast EGaIn–PBMA hybrid

LETTERS NATURE NANOTECHNOLOGY

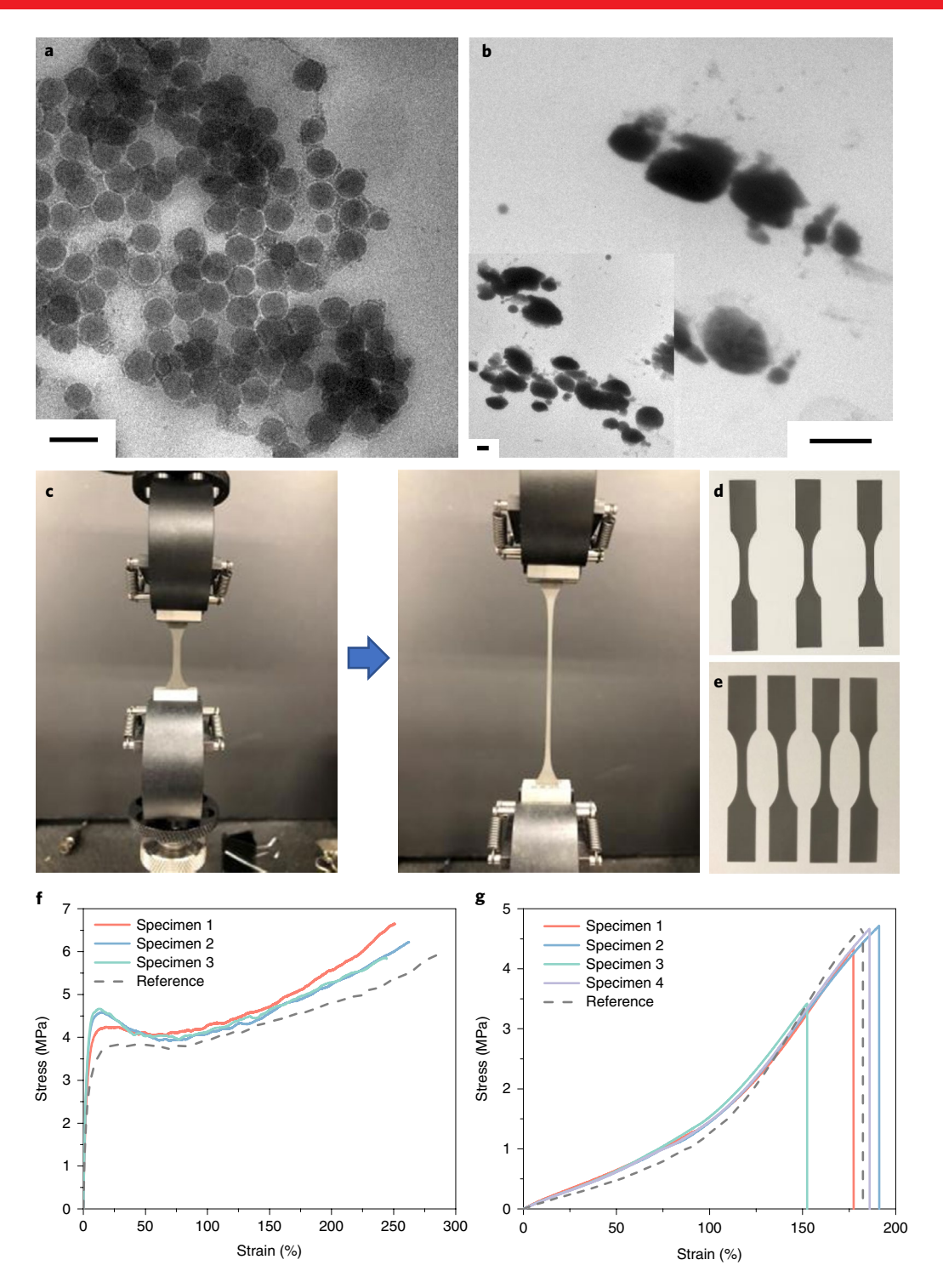


Fig. 2 | EGaln-PBMA hybrid droplets and their tensile performances. a, TEM image of the supernatant of the EGaln-PBMA dispersion in tetrahydrofuran after settling for 24 h. Scale bar, 200 nm. **b**, Microtomic TEM images of as-cast EGaln-PBMA specimens from a tetrahydrofuran dispersion. Scale bars, 200 nm. **c**, Photographs showing tensile test of a specimen of EGaln-PBMA at 5 mm min⁻¹. **d,f**, As-cast Type V (ASTM D638) specimens of EGaln-PBMA (**d**) and corresponding stress-strain profiles (**f**) with a 20.0 mm gauge length. The pure PBMA specimen is shown as a grey dashed line. **e,g**, As-cast Type V (ASTM D638) specimens of EGaln-PBMA incorporated into Sylgard 184 resin at a 10:1 (wt/wt) ratio (**e**) and the corresponding stress-strain profiles (**g**) with a 20.0 mm gauge length. The pure Sylgard specimen is shown as grey dashed line.

material was a tough elastomer with an average elastic modulus of $73\pm7\,\mathrm{MPa}$ and a maximal tensile strain of $\sim\!238\pm40\%$ before failure (Fig. 2c,f). The modulus and mechanical strength of the EGaIn-PBMA specimen were slightly larger than those of the pure PBMA ($M_{\rm n}\!=\!3.0\!\times\!10^5$) reference specimen, probably due to the

contribution of the surface tension of the liquid metal¹³. Nonetheless, the change in stress–strain response is modest and suggests that the liquid-phase droplets do not have a significant influence on the stiffness or strain limit of the polymer matrix. Note that the direct processing of polymer-tethered nanodroplets into hybrid materials

LETTERS

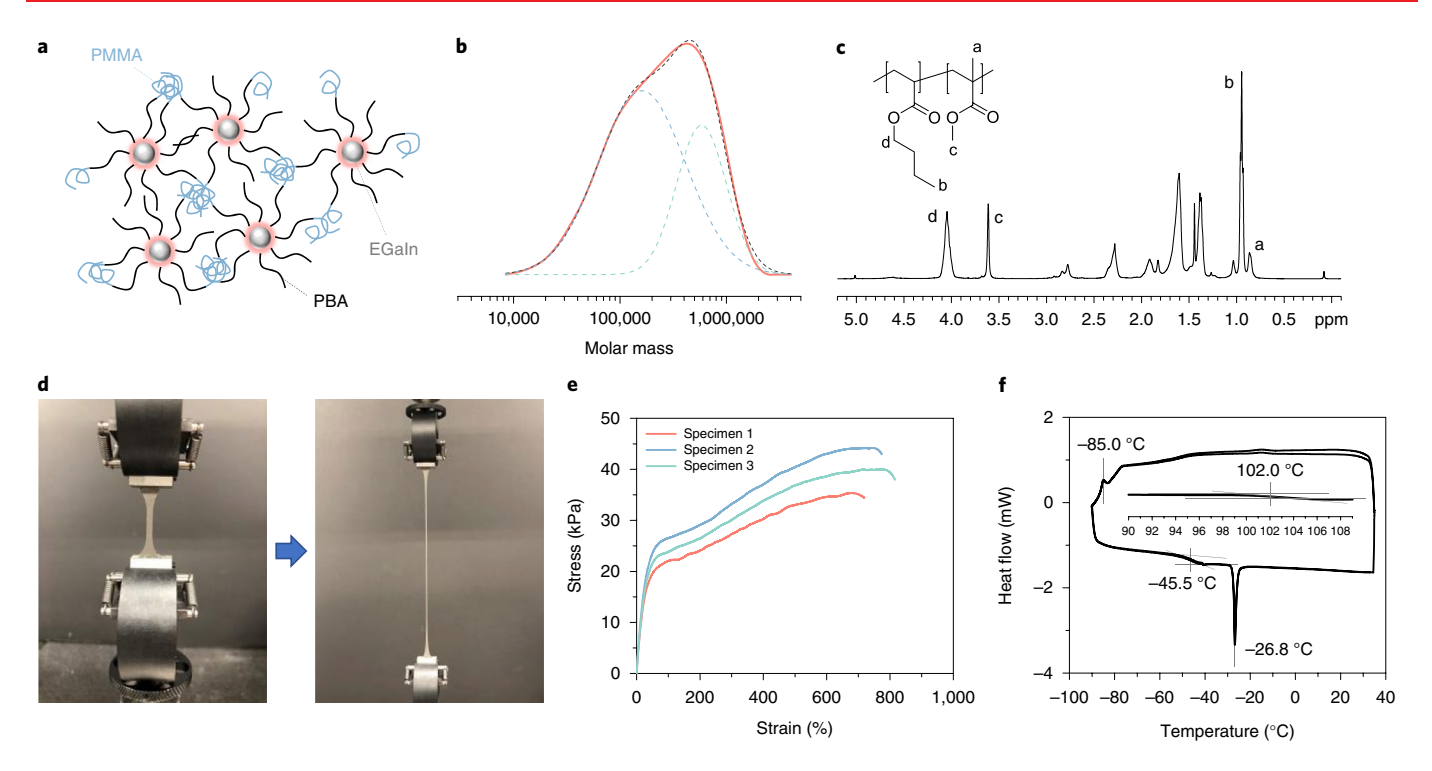


Fig. 3 | EGaIn-PBA-b-PMMA thermoplastic elastomer. **a**, Illustration of PMMA-b-PBA-grafted EGaIn hybrid materials physically crosslinked by glassy PMMA moieties (blue), while the fluid PBA chains (black) and EGaIn droplets (grey) provide the dynamic mechanical properties to the matrix. **b**, Size exclusion chromatography (SEC) traces of detached PMMA-b-PBA showing partial extension of PMMA from the PBA-Br macroinitiator (solid red line) and the corresponding deconvoluted peaks of PBA-Br (blue dashed line) and PBA-b-PMMA (cyan dashed line) assuming Gaussian distribution of the peaks on a differential refractive index versus elution timescale. The grey dashed line resembles the sum of the two deconvoluted peaks. **c**, ¹H NMR spectrum of PMMA-b-PBA-grafted EGaIn hybrid materials in CDCl₃. The molar ratio between MMA and BA units was calculated by integration of peaks c and d: $r_{\text{NMA/BA}} = 3/2 \times I_{\text{c}}/I_{\text{d}}$. **d**, **e**, Photographs showing tensile test of a PMMA-b-PBA-grafted EGaIn hybrid material specimen (Type V, ASTM D638) at 5 mm min⁻¹ (**d**) and the corresponding stress-strain profiles with a 20.0 mm gauge length (**e**). **f**, DSC curve of PMMA-b-PBA-grafted EGaIn hybrid materials. Inset, section of the DSC curve of a separate scan with a temperature range covering the T_{e} of PMMA.

alleviates the need for compatibilization (which is a major challenge for typical composites based on mixtures of components). It also enables the stabilization of high volume fractions of inorganic component; for example, the sample presented in Fig. 2 contains 31.2 wt% (~6.5 vol%) EGaIn.

Inorganic particles grafted with PBMA brushes with a high molecular weight displayed a moderate compatibility with silicone-based elastomers 20 . Therefore, EGaIn–PBMA hybrid materials were mixed with a silicone-based elastomer. Photo-images of the as-cast specimen confirmed a good compatibility of the EGaIn–PBMA hybrid with the Sylgard 184 matrix at a 10:1 (wt/wt) ratio (Fig. 2g). As the covalently crosslinked silicone matrix did not allow much stress relaxation, no yielding was displayed before failure. A low failure strain of $176\pm17\%$ was observed. The average elastic modulus of $1.52\pm0.07\,\mathrm{MPa}$ was within the typical range of Sylgard 184 and comparable to the reference specimen (Fig. 2g) 21 , suggesting that the use of liquid-phase inclusions preserves the mechanical properties of the host polymer.

Thermoplastic elastomers typically consist of ABA triblock copolymers, with two crystalline or glassy A blocks acting as a physical crosslinker after microphase separation, and a B block that forms a soft continuous elastic matrix 22 . The material becomes processable when the temperature is above the $T_{\rm g}$ of the crosslinking blocks or order–disorder transition temperature. Star polymers with PBA-b-PMMA arms have been demonstrated to be good thermoplastic elastomers 23 .

Consequently, PBA was initially grafted from the EGaIn droplet surface via one-pot supplemental activator and reducing agent ATRP (Table 1, entry 4). However, because the PBA-Br chain-ends were less reactive than the PMMA-Br chain-ends, only a fraction of the PBA-Br chain-ends were initiated to allow chain extension with MMA, causing a bimodal distribution of molecular weight (Fig. 3a,b)²⁴. The extended chains contributed to the formation of physical crosslinking, while the unreacted chains provided entanglement of PBA arms. The molar ratio between MMA and BA units in the purified sample was determined to be 21.7/78.3.

Like EGaIn–PBMA hybrid materials, the EGaIn–PBA-b-PMMA hybrid material was solvent-cast into dog-bone-shaped specimens from a tetrahydrofuran dispersion. The specimen was much softer and stickier than the EGaIn–PBMA hybrid materials. The average elastic modulus of the samples measured at 5% strain was 89 kPa. A high elongation of $769 \pm 49\%$ was achieved in this sample due to a synergic contribution from the dynamic PBA and EGaIn contents and slippage of the physical crosslinked PMMA microdomains. The much lower elastic modulus of 89 ± 6 kPa was primarily caused by the high PBA and EGaIn content (65.6 and 20.2 wt%, respectively).

The thermal transitions of the material were examined by differential scanning calorimetry (DSC) (Fig. 3f). The $T_{\rm g}$ of PBA was observed at $-45.5\,^{\circ}$ C. To observe the $T_{\rm g}$ of PMMA, a separate scan with higher sample loading was performed and the curve was locally magnified. Interestingly, a significant suppression of crystallization and melting point of EGaIn was also observed. Crystallization of EGaIn did not occur until the temperature reached below $-85\,^{\circ}$ C and the melting temperature was reduced to $-26.8\,^{\circ}$ C. This observation can be correlated with previous reports of size-dependent crystallization and melting points of metal nanoparticles^{25–27}.

LETTERS NATURE NANOTECHNOLOGY

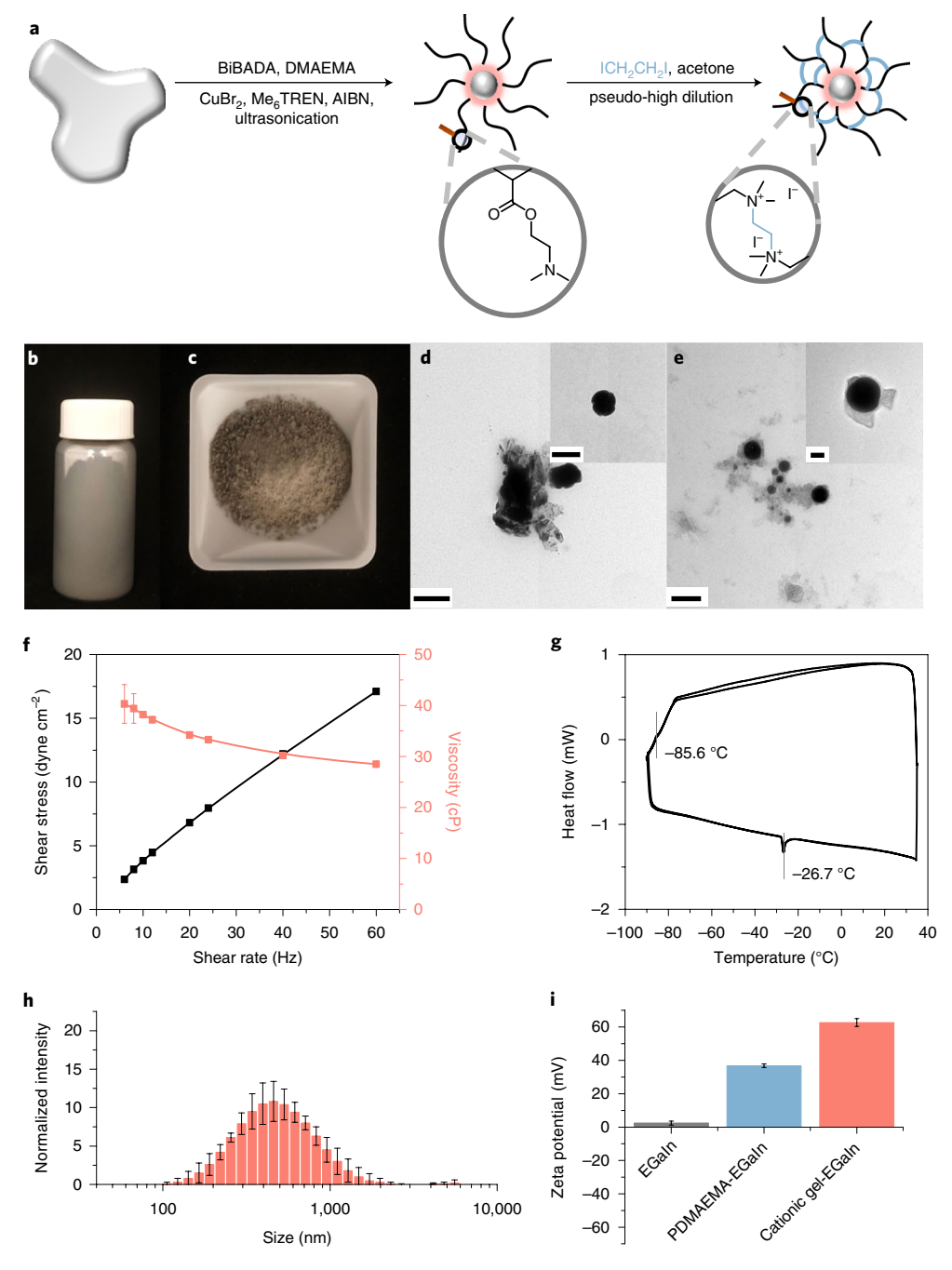


Fig. 4 | EGaIn-PDMAEMA water-soluble hybrid droplets and cationic gel-wrapped EGaIn. **a**, Synthetic scheme. BiBADA, 12-(2-bromoisobutyramido) dodecanoic acid; DMAEMA, 2-(dimethylamino)ethyl methacrylate; Me₆TREN, tris(2-(dimethylamino)ethyl)amine; AIBN, 4,4'-azobisisobutyronitrile. **b,c**, Photographs of EGaIn-PDMAEMA as a film with metallic lustre after drying at 3,000-8,000 r.p.m. in vacuo (**b**) and cationic gel-wrapped EGaIn (**c**). **d**, TEM images of EGaIn-PDMAEMA. Scale bars, 500 nm and 200 nm (inset). **e**, TEM images of cationic gel-wrapped EGaIn. Scale bars, 100 nm. **f**, Shear stress and viscosity of a 2.0 wt% dispersion of cationic gel-wrapped EGaIn droplets in water. **g**, DSC curve of cationic gel-wrapped EGaIn. **h**, Intensity-weighted hydrodynamic size distribution of cationic gel-wrapped EGaIn in a 1 mg ml⁻¹ aqueous dispersion. **i**, Zeta potential of EGaIn (grey, 2.4 ± 1.2 mV), EGaIn-PDMAEMA hybrid (blue, 36.8 ± 1.1 mV) and cationic gel-wrapped EGaIn (red, 62.7 ± 2.4 mV) in 1 mg ml⁻¹ aqueous dispersions. All error bars represent standard deviation (**f,h,i**).

The suppression of the melting temperature was demonstrated in liquid metal dispersions. This finding might be of interest, for example, for the design of actuating materials in soft robotics that are to retain their properties in low-temperature environments.

Hydrophilic polymer brushes, such as PDMAEMA, were also grafted from EGaIn droplets, enabling water dispersibility (Table 1). To further improve its water dispersibility and restrain

the aggregation of EGaIn droplets, the polymer chains were cross-linked by reacting the ubiquitous dimethylamino pendant groups with an excess of 1,2-diiodoethane under pseudo-high-dilution conditions (Fig. 4a)²⁸. As a result, a cationic gel-wrapped EGaIn was synthesized.

The EGaIn-PDMAEMA hybrid material formed a grey film with slight metallic lustre in the vial after the solvent was removed

NATURE NANOTECHNOLOGY LETTERS

(Fig. 4b). However, after crosslinking the film-forming ability of the material was eliminated, and a grey powder was obtained (Fig. 4c). TEM shows irregular shapes of the EGaIn droplets formed after grafting PDMAEMA brushes from the surface, which is likely due to competitive surface attachment of the amino groups (Fig. 4d). However, a fraction of spherical droplets was also detected. In contrast, when the PDMAEMA brushes were crosslinked, almost all droplets became spherical but with a broad size distribution (Fig. 4e). The cationic gel, with a high iodide content, was observed around the EGaIn droplets in the TEM images. Although the gelwrapped EGaIn droplets lost film-forming ability, it showed friction in an aqueous dispersion, behaving similarly to particle dispersions²⁹. The viscosity reached 2.26 ± 0.23 cP (0.5 wt% aq.). The rheological study demonstrated the shear thinning behaviour of the aqueous dispersion (Fig. 4f), probably due to separation of the gels originally bridged by iodide counterions. The presence of crystallization and melting peaks in the DSC traces (Fig. 4g) confirms the composition of the gel-coated EGaIn nanodroplets; however, because of the reduced EGaIn content in the gel hybrid (Table 1), the peaks are not as prominent as in the polymer/EGaIn hybrid materials shown in Fig. 3f.

The aqueous dispersion of the cationic gel-wrapped EGaIn showed a rather broad hydrodynamic size distribution (Fig. 4h) due to droplet size distribution and inevitable inter-droplet crosslinking that occurred when the EGaIn-PDMAEMA dispersion was added to the 1,2-diiodoethane solution, as also shown in the TEM images. The zeta potentials of EGaIn, EGaIn-PDMAEMA hybrid and cationic gel-wrapped EGaIn in each of their aqueous dispersions were measured to compare the properties of the materials in each stage (Fig. 4i). Note that the pristine EGaIn does not form a stable dispersion at this concentration. A small positive charge of $2.4 \pm 1.2 \,\mathrm{mV}$ was observed for the pristine EGaIn aqueous dispersion, probably due to partial ionization of the oxide layer. The EGaIn-PDMAEMA hybrid became more positive as the amine side groups were protonated in water. Because the cationic gel-wrapped EGaIn had a high content of quaternized amine, it carried a high positive potential of $62.7 \pm 2.4 \,\text{mV}$.

We have shown the preparation of a series of EGaIn-polymer hybrid materials via SI-ATRP from a liquid metal oxide surface functionalized by BiBADA. The application of SI-ATRP from a liquid metal has enabled the synthesis of one-component polymer/EGaIn hybrid materials with well-defined microstructure possessing fortuitous property combinations. Polymer-tethered EGaIn nanodroplets display a significant reduction of the EGaIn solidification temperature and can be incorporated within polymeric materials with glass transition temperatures above and below room temperature, allowing preparation of a diverse range of EGaIn-polymer hybrid materials with high stability, excellent dispersibility and tunable mechanical and optical properties. Additional research in this area can potentially lead to on-demand development of new materials with liquid metal for future soft electronics.

Online content

Any methods, additional references, Nature Research reporting summaries, source data, statements of data availability and associated accession codes are available at https://doi.org/10.1038/s41565-019-0454-6.

Received: 25 November 2018; Accepted: 11 April 2019; Published online: 20 May 2019

References

 Bartlett, M. D. et al. High thermal conductivity in soft elastomers with elongated liquid metal inclusions. *Proc. Natl Acad. Sci. USA* 114, 2143–2148 (2017). Fassler, A. & Majidi, C. Liquid-phase metal inclusions for a conductive polymer composite. Adv. Mater. 27, 1928–1932 (2015).

- Kramer, R. K., Majidi, C. & Wood, R. J. Masked deposition of gallium-indium alloys for liquid-embedded elastomer conductors. *Adv. Funct. Mater.* 23, 5292–5296 (2013).
- Tabatabai, A., Fassler, A., Usiak, C. & Majidi, C. Liquid-phase galliumindium alloy electronics with microcontact printing. *Langmuir* 29, 6194–6200 (2013).
- Palleau, E. et al. Self-healing stretchable wires for reconfigurable circuit wiring and 3D microfluidics. Adv. Mater. 25, 1589–1592 (2013).
- Blaiszik, B. J. et al. Autonomic restoration of electrical conductivity. *Adv. Mater.* 24, 398–401 (2012).
- Markvicka, E. J., Bartlett, M. D., Huang, X. & Majidi, C. An autonomously electrically self-healing liquid metal-elastomer composite for robust soft-matter robotics and electronics. *Nat. Mater.* 1, 618–624 (2018).
- Kumar, S. K., Benicewicz, B. C., Vaia, R. A. & Winey, K. I. 50th anniversary perspective: are polymer nanocomposites practical for applications? *Macromolecules* 50, 714–731 (2017).
- Finkenauer, L. R. et al. Analysis of the efficiency of surfactant-mediated stabilization reactions of EGaIn nanodroplets. *Langmuir* 33, 9703–9710 (2017).
- Farrell, Z. J. & Tabor, C. Control of gallium oxide growth on liquid metal eutectic gallium/indium nanoparticles via thiolation. *Langmuir* 34, 234–240 (2018).
- 11. Hohman, J. N. et al. Directing substrate morphology via self-assembly: ligand-mediated scission of gallium-indium microspheres to the nanoscale. *Nano Lett.* **11**, 5104–5110 (2011).
- Boley, J. W., White, E. L. & Kramer, R. K. Mechanically sintered galliumindium nanoparticles. Adv. Mater. 27, 2355–2360 (2015).
- Dickey, M. D. et al. Eutectic gallium-indium (EGaIn): a liquid metal alloy for the formation of stable structures in microchannels at room temperature. Adv. Funct. Mater. 18, 1097–1104 (2008).
- Yan, J. et al. A fatty acid-inspired tetherable initiator for surface-initiated atom transfer radical polymerization. *Chem. Mater.* 29, 4963–4969 (2017).
- Xu, Q. et al. Effect of oxidation on the mechanical properties of liquid gallium and eutectic gallium-indium. Phys. Fluids 24, 063101 (2012).
- Konkolewicz, D. et al. SARA ATRP or SET-LRP. End of controversy? Polym. Chem. 5, 4396–4417 (2014).
- Chung, J. Y., Nolte, A. J. & Stafford, C. M. Surface wrinkling: a versatile platform for measuring thin-film properties. Adv. Mater. 23, 349–368 (2011).
- 18. Brandrup J. et al. (eds) Polymer Handbook 4th edn (Wiley, 1999).
- Porter, R. S. & Johnson, J. F. The entanglement concept in polymer systems. Chem. Rev. 66, 1–27 (1966).
- Wahlander, M. et al. Tailoring dielectric properties using designed polymergrafted ZnO nanoparticles in silicone rubber. *J. Mater. Chem. A* 5, 14241–14258 (2017).
- Johnston, I., McCluskey, D., Tan, C. & Tracey, M. Mechanical characterization of bulk Sylgard 184 for microfluidics and microengineering. J. Micromech. Microeng. 24, 035017 (2014).
- Spontak, R. J. & Patel, N. P. Thermoplastic elastomers: fundamentals and applications. Curr. Opin. Colloid Interface Sci. 5, 333–340 (2000).
- Dufour, B., Koynov, K., Pakula, T. & Matyjaszewski, K. PBA-PMMA 3-arm star block copolymer thermoplastic elastomers. *Macromol. Chem. Phys.* 209, 1686–1693 (2008).
- Yan, J. et al. Matrix-free particle brush system with bimodal molecular weight distribution prepared by SI-ATRP. Macromolecules 48, 8208–8218 (2015).
- Dick, K., Dhanasekaran, T., Zhang, Z. & Meisel, D. Size-dependent melting of silica-encapsulated gold nanoparticles. J. Am. Chem. Soc. 124, 2312–2317 (2002).
- Wronski, C. R. M. The size dependence of the melting point of small particles of tin. Br. J. Appl. Phys. 18, 1731 (1967).
- Yamaguchi, A., Mashima, Y. & Iyoda, T. Reversible size control of liquidmetal nanoparticles under ultrasonication. *Angew. Chem. Int. Ed.* 54, 12809–12813 (2015).
- 28. Rossa, L. & Vögtle, F. in *Cyclophanes I* Vol. 113 (ed Vögtle, F.) 1–86 (Springer, 1983).
- Mansfield, M. L., Douglas, J. F., Irfan, S. & Kang, E.-H. Comparison of approximate methods for calculating the friction coefficient and intrinsic viscosity of nanoparticles and macromolecules. *Macromolecules* 40, 2575–2589 (2007).

Acknowledgements

The authors acknowledge financial support from the National Science Foundation (DMR 1501324, DMR-1709344 and CMMI-1663305) and the Air Force Office of Scientific Research (AFOSR) Multidisciplinary University Research Initiative (FA9550-18-1-0566; programme manager, K.Goretta). The authors also acknowledge the use of facilities in the Colloids, Surfaces and Polymer Laboratory at Carnegie Mellon, supported by grant no. CMU 678083-769798.

LETTERS NATURE NANOTECHNOLOGY

Author contributions

J.Y. and M.H.M. conceived and designed the experiments. J.Y. performed the synthesis and kinetic studies. J.Y., M.H.M. and Z.L. fabricated and characterized the materials. Z.W. performed the microscopic characterization. N.K. and C.P. were involved in discussions at various stages of the work. M.R.B., C.M. and K.M. supervised the work. All authors discussed the results and commented on the manuscript.

Competing interests

The authors declare no competing interests.

Additional information

Supplementary information is available for this paper at $\rm https://doi.org/10.1038/s41565-019-0454-6.$

Reprints and permissions information is available at www.nature.com/reprints.

Correspondence and requests for materials should be addressed to M.R.B., C.M. or K.M.

Publisher's note: Springer Nature remains neutral with regard to jurisdictional claims in published maps and institutional affiliations.

© The Author(s), under exclusive licence to Springer Nature Limited 2019

NATURE NANOTECHNOLOGY LETTERS

Methods

Materials. Copper bromide (CuBr₂, Aldrich, 99%), indium (Alfa, 99.9995%), gallium (Alfa, 99.9%), 1,2-diiodoethane (TCI, 97%), tris[2-(dimethylamino)ethyl] amine (Me₆TREN, Koei, 99%), N,N,N',N'',N''-pentamethyldiethylenetriamine (PMDETA, Aldrich, 99%), ethyl 2-bromoisobutyrate (EBiB, Aldrich, 98%), hydrochloric acid (HCl, Fisher, 36.5-38.0%), 4,4'-azobis(4-cyanovaleric acid) (V-501, Wako), anisole (Aldrich, 99%), tetrahydrofuran (EMD, 99.5%), acetone (EMD, 99.5%), methanol (EMD, 99.8%), acetonitrile (MeCN, Fisher, 99.5%) and dimethylformamide (Fisher, 99.8%) were used as received. 2,2'-Azobisisobutyronitrile (AIBN, Aldrich, 98%) was recrystallized from ethanol following literature procedures30. Methyl methacrylate (MMA, Aldrich, 99%), n-butyl acrylate (BA, Acros, 99%), 2-(dimethylamino)ethyl methacrylate (DMAEMA, Aldrich, 98%) and n-butyl methacrylate (BMA, Aldrich, 99%) were purified by elution through a basic alumina column. Deionized (DI) water was collected from a Millipore Milli-Q water purification system. 12-(2-Bromoisobutyramido)dodecanoic acid (BiBADA) was synthesized according to a literature procedure 14. A linear PBMA reference sample was synthesized via conventional radical polymerization at 60 °C using 10 vol% of anisole as solvent and 0.5 mol% of AIBN as radical initiator.

Characterization. The number-average molecular weight (M_n) and dispersity $(M_{\rm w}/M_{\rm n})$ were determined by SEC. Polymer-grafted EGaIn droplets were dispersed in tetrahydrofuran and treated with HCl before SEC analysis. The SEC was conducted with a Waters 515 pump and Waters 410 differential refractometer using PSS columns (Styrogel 105, 103, 102 Å) in tetrahydrofuran as an eluent at 35 °C and at a flow rate of 1 ml min⁻¹. Linear PMMA standards were used for SEC calibration. ¹H NMR spectroscopy was performed on a Bruker Avance 300 MHz spectroscope with CDCl₃ as the solvent. Conversion was calculated by following the decrease of the monomer peak area relative to the peak areas of the methoxy protons. The hydrodynamic size distribution of the polymer-grafted nanoparticles was determined by a Malvern Zetasizer Nano ZS particle size analyser. TGA was performed on a TA Instrument TGA 2950 and data were processed with TA Universal Analysis software. The heating procedure involved four steps: (1) ramp up at 20 °C min⁻¹ to 120 °C, (2) hold at 120 °C for 20 min, (3) high-resolution ramp up at 20 °C min⁻¹ to 800 °C, (4) hold at 800 °C for 10 min. The organic content of the samples was normalized to the weight loss between 120 and 800 °C. The inorganic content was then corrected by the molecular weight of gallium and indium oxides. The DSC measurements were performed on a TA Instruments Q20 DSC. Specimens were prepared by drop-casting nanocomposite solutions into Tzero aluminium pans. Before the experiment, the removal of solvent was performed at room temperature and followed by heating the pan to 100 °C. For DSC runs, 5-10 mg specimens were cooled to -90 °C and then heated to 35 °C at a rate of 10 °C min⁻¹ under a constant flow (50 ml min⁻¹) of nitrogen. TEM was performed using a JEOL EX2000 electron microscope operated at 200 kV. Images were taken by amplitude and phase contrast using a Gatan Orius SC600 high-resolution camera. The rheology at different shear rates was measured by a Brookfield Model DVII + PRO cone and plate viscometer with a CPE-41 cone. A 2 ml volume of the aqueous dispersion was transferred into the cup and a Brookfield TC-602 water bath was used to keep the cup at 25 °C. The shear rate was increased from 0.5 to 100 s⁻¹. The torque, shear stress, viscosity and the error of viscosity measured as 1% of maximum viscosity at 100% torque were read at each shear rate. To ensure the accuracy of the measurement, we only used the data with torque values between 10 and 100%.

Eutectic gallium indium alloy. To make eutectic gallium indium alloy with $75.5 \, \text{wt}\%$ Ga and $24.5 \, \text{wt}\%$ In, $50.0 \, \text{g}$ of as-received gallium was first melted at $50 \, ^{\circ}\text{C}$ in a $50 \, \text{ml}$ beaker. The melted Ga was then added to $16.2 \, \text{g}$ of indium shots. The melted Ga and In were stirred at $190 \, ^{\circ}\text{C}$ for several hours. The liquid EGaIn alloy was brought back to room temperature on the hotplate and stored in a closed container.

Typical procedures of polymerization. Kinetic study. EGaIn (2.0 g, 0.32 ml) was mixed with 40.0 mg (110 μ mol) of BiBADA and 4.7 ml of anisole. The mixture was ultrasonicated overnight. CuBr₂ (2.4 mg, 11 μ mol), 14.7 μ l (54.8 μ mol) of Me₆TREN (or 11.5 μ l of PMDETA), 4.7 ml (44 mmol) of MMA and 5.4 mg (33 μ mol) of AIBN were added. In the initial experiment, CuBr₂, Me₆TREN and MMA were added before ultrasonication. The reaction was degassed by nitrogen bubbling. The reaction was stirred at 50 °C for 4 or 8 h. An aliquot of the sample was taken at various time intervals to monitor the molecular weights and monomer conversions.

Stepwise synthesis of EGaIn–PMMA hybrid materials. EGaIn (1.0g) and 0.8 g (2.2 mmol) of BiBADA were mixed in 10 ml tetrahydrofuran and sonicated at room temperature overnight. The initiator-modified EGaIn droplets were washed by

tetrahydrofuran in three sonication—centrifugation cycles as a grey viscous fluid. The EGaIn droplets were then dispersed in 2.7 ml (25 mmol) of MMA and 2.7 ml of anisole. CuBr $_2$ (28.5 µl, 20.0 mg ml $^{-1}$, 2.54 µmol) and 1.3 µl of Me $_6$ TREN were added. The reaction was degassed by nitrogen bubbling. A Ø1 mm \times 1 cm copper wire was added to the reaction. The reaction was allowed to proceed at room temperature in a sonication bath until reaching a desired conversion. The polymer was purified by precipitation in methanol.

One-pot synthesis. EGaIn (0.5 g, 80 μ l), 10 mg (27 μ mol) of BiBADA, 3.0 ml (27 mmol) of MMA (or 4.4 ml, 27 mmol of BMA), 30.5 μ l of 20.0 mg ml $^{-1}$ (2.74 μ mol) CuBr $_2$ and 3.7 μ l (14 μ mol) of Me $_6$ TREN were mixed with an equivalent volume of anisole in a Schlenk flask. The mixture was ultrasonicated overnight, then 2.3 mg (14 μ mol) of AIBN was added. The reaction was degassed by nitrogen bubbling. The reaction was allowed to proceed at 50 °C in a sonication bath until reaching a desired conversion. The polymer was purified by precipitation in methanol.

EGaIn (1.0 g, 0.16 ml), 20 mg (55 $\mu mol)$ of BiBADA, 3.7 ml (22 mmol) of DMAEMA, 61 μl of 20.0 mg ml $^{-1}$ (5.5 $\mu mol)$ CuBr $_2$ and 7.4 μl (27 $\mu mol)$ of Me $_6$ TREN were mixed with 3.7 ml of MeCN in a Schlenk flask. The mixture was ultrasonicated overnight. V-501 (4.6 mg, 16 μmol) was added. The reaction was degassed by nitrogen bubbling. The reaction was allowed to proceed at 50 °C in a sonication bath until reaching a desired conversion. The polymer was purified by dialysis against methanol.

EGaIn–PBA-b-PMMA. EGaIn (2.0 g, 320 μl), 40 mg (0.11 mmol) of BiBADA, 15.8 ml (110 mmol) of BA, 2.5 mg (11 μmol) CuBr₂ and 14.7 μl (54.8 μmol) of Me₆TREN were mixed with 15.8 ml of anisole in a Schlenk flask. The mixture was ultrasonicated overnight. The reaction was degassed by nitrogen bubbling. A 01 mm × 1 cm copper wire was added to the reaction. The reaction was allowed to proceed at room temperature in a sonication bath until reaching a desired conversion. The polymer was purified by dialysis against methanol. EGaIn–PBA (8.0 g) was dispersed in 4.4 ml (41 mmol) of MMA and 13.1 ml of anisole, then 91 μl of 20.0 mg ml $^{-1}$ (8.1 μmol) CuBr₂, 10.9 μl (41 μmol) of Me₆TREN and 6.7 mg (41 μmol) of AIBN were added. The reaction was degassed by nitrogen bubbling. The reaction was allowed to proceed at 50 °C in a sonication bath until reaching a desired conversion. The polymer was purified by dialysis against methanol.

Crosslinking PDMAEMA brushes. EGaIn–PDMAEMA (1.7 g) was dispersed in 100 ml of acetone and added dropwise into a solution of 2.15 g (16.2 mmol) of 1,2-diiodoethane in 50 ml of acetone under vigorous stirring. The mixture was stirred overnight and purified by dialysis against methanol and water.

Free-standing film preparation. The PMMA-grafted EGaIn droplets were dispersed in tetrahydrofuran via ultrasonication and stirring. The resulted dispersion was settled for 3 days and the supernatants were transferred into a 1.2-in-diameter cylindrical Teflon mould. A semi-transparent, free-standing film was obtained after the solvent was slowly evaporated over 48 h at room temperature. Before electron imaging, the films were microsectioned with a thickness of 70 nm at $-120\,^{\circ}\text{C}$ using a LEICA EM FCS cryo-ultramicrotome.

Solution casting was used to fabricate free-standing films for embedded EGaIn micro-/nanoparticles in PBA-b-PMMA and PBMA polymers as well as EGaIn-PBMA-elastomer. For PBA-b-PMMA and PBMA films, the synthesized polymer was dissolved in tetrahydrofuran with a weight ratio of 1:5 (polymer/solvent). The solution was then cast onto a metal plate, which was sprayed with a mould release (Smooth-On Universal Mould Release). The film was then covered with a Petri dish to lower the evaporation rate of tetrahydrofuran and eliminate the formation of surface bubbles at room temperature. Next, the films were heated at 60 °C for 2 h before being cut into desired geometries. To prepare EGaIn-PBMA-elastomer hybrid materials, acetone was used as the solvent to dissolve the EGaIn-PBMA polymer; this was then mixed with Sylgard 184 in a mixed ratio of 1:10. After evaporating the solvent at room temperature, the elastomer was cured at 100 °C for 1 h. Once the films were prepared, tensile test specimens in the shape of a dog bone were cut using a laser cutter (VLS 3.50, Universal Laser Systems).

Data availability

The data that support the plots within this paper and other findings of this study are available from the corresponding author on reasonable request.

References

 Tsuda, K., Kobayashi, S. & Otsu, T. Vinyl polymerization. CXVI. The effects of several sulfides and oxides on radical polymerization. *Bull. Chem. Soc. Jpn* 38, 1517–1522 (1965).